

# A $\beta$ -Boronopeptide Bundle of Known Structure As a Vehicle for Polyol Recognition

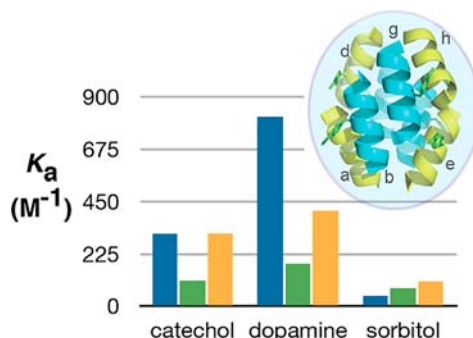
Michael S. Melicher,<sup>†</sup> John Chu,<sup>†</sup> Allison S. Walker,<sup>†</sup> Scott J. Miller,<sup>\*,†</sup>  
Richard H. G. Baxter,<sup>\*,†,‡</sup> and Alanna Schepartz<sup>\*,†,§</sup>

Department of Chemistry, Department of Molecular Biophysics and Biochemistry,  
and Department of Molecular, Cellular and Developmental Biology, Yale University,  
New Haven, Connecticut 06520-8107, United States

Alanna.schepartz@yale.edu; richard.baxter@yale.edu; scott.miller@yale.edu

Received August 20, 2013

## ABSTRACT



Despite significant progress in the design of receptors and sensors for simple polyols and monosaccharides, few synthetic receptors discriminate among multiple saccharide units simultaneously, especially under physiological conditions. Described here is the three-dimensional structure of a supramolecular complex—a  $\beta$ -peptide bundle—designed for the potential to interact simultaneously with as many as eight discrete monosaccharide units. The preliminary evaluation of this construct as a vehicle for polyol binding is also presented.

Carbohydrates encode chemical information in a language defined by stereochemically distinct arrays of hydroxyl functionality arranged on hydrophobic skeletons. Natural carbohydrates can be as small as glyceraldehyde ( $90 \text{ g} \cdot \text{mol}^{-1}$ ) and as large as hyaluronan ( $> 10^6 \text{ g} \cdot \text{mol}^{-1}$ ); the average N-glycan comprises between 10 and 12 monosaccharide units arranged in linear and branched arrays.<sup>1</sup> Receptors for saccharides in nature, proteins known as lectins, employ two general strategies to decode the information contained in a complex sugar: networks of hydrogen bonds coordinate hydroxyl groups, and  $\text{CH}-\pi$  and van der Waals interactions interact with the

hydrocarbon backbone.<sup>2</sup> There has been much work over the years on the design of synthetic receptors<sup>3–9</sup> and sensors<sup>8,10–15</sup> for simple polyols and saccharides, many of which rely on the highly favorable interaction of polyols

(3) Sookcharoenpinyo, B.; Klein, E.; Ferrand, Y.; Walker, D. B.; Brotherhood, P. R.; Ke, C.; Crump, M. P.; Davis, A. P. *Angew. Chem., Int. Ed.* **2012**, *51*, 4586.

(4) Ke, C.; Destecroix, H.; Crump, M. P.; Davis, A. P. *Nat. Chem.* **2012**, *4*, 718.

(5) Bicker, K. L.; Sun, J.; Lavigne, J. J.; Thompson, P. R. *ACS Comb. Sci.* **2011**, *13*, 232.

(6) Hargrove, A. E.; Ellington, A. D.; Anslyn, E. V.; Sessler, J. L. *Bioconjugate Chem.* **2011**, *22*, 388.

(7) Davis, A. P. *Org. Biomol. Chem.* **2009**, *7*, 3629.

(8) Mazik, M. *Chem. Soc. Rev.* **2009**, *38*, 935.

(9) Duggan, P. J.; Offermann, D. A. *Tetrahedron* **2009**, *65*, 109.

(10) Bull, S. D.; Davidson, M. G.; Van den Elsen, J. M. H.; Fossey, J. S.; Jenkins, A. T. A.; Jiang, Y.-B.; Kubo, Y.; Marken, F.; Sakurai, K.; Zhao, J.; James, T. D. *Acc. Chem. Res.* **2013**, *46*, 312.

(11) Huang, S.; Jia, M.; Xie, Y.; Wang, J.; Xu, W.; Fang, H. *Curr. Med. Chem.* **2012**, *19*, 2621.

(12) Martinez, A.; Ortiz Mellet, C.; Garcia Fernandez, J. M. *Chem. Soc. Rev.* **2013**, *42*, 4746.

<sup>†</sup> Department of Chemistry.

<sup>‡</sup> Department of Molecular Biophysics and Biochemistry.

<sup>§</sup> Department of Molecular, Cellular and Developmental Biology.

(1) Varki, A.; Cummings, R. D.; Esko, J. D.; Freeze, H. H.; Stanley, P.; Bertozzi, C. R.; Hart, G. W.; Etzler, M. E. *Essentials of Glycobiology*, 2nd ed.; Cold Spring Harbor Laboratory Press: New York, 2009.

(2) Arnaud, J.; Audfray, A.; Imberty, A. *Chem. Soc. Rev.* **2013**, *42*, 4798.

with boronic acids.<sup>16</sup> Despite significant progress in the context of mono- and simple disaccharides,<sup>3,17–19</sup> there are few examples of synthetic receptors that interact with complex oligosaccharides, especially in aqueous solution.<sup>4,18,20</sup> Indeed, the issue of multivalency—the embodiment of multiple, directional, and reversible interactions—is a signature component of biological binding events,<sup>21,22</sup> as well as enzymatic and abiological catalysis.<sup>23</sup> In this work we describe the high-resolution structure of a supramolecular complex, a  $\beta$ -peptide bundle, with eight potential saccharide binding sites. Also presented is the preliminary evaluation of this construct as a polyol complexation vehicle.

$\beta$ -Peptide bundles comprise a family of supramolecular complexes that self-assemble spontaneously from short  $\beta$ -peptide monomers into well folded and thermostable structures.  $\beta$ -Peptides that form bundles assemble into 14-helices with three faces: a hydrophobic face whose residues contribute to the characteristic bundle core, a salt bridge face whose residues contribute to aqueous solubility and bundle stability, and an aromatic face whose residues interact with solvent (Figure 1).  $\beta$ -Peptide bundles are unique among foldamers and supramolecules in that their kinetic and thermodynamic signatures resemble those of natural proteins.<sup>24–27</sup> The most thermodynamically stable  $\beta$ -peptide bundle reported, an octamer of the  $\beta$ -peptide dodecamer Zwit-EYYK, is 90% assembled at a monomer concentration of 15  $\mu$ M. The atomic structure of the Zwit-EYYK octamer has been determined.<sup>27</sup> Each Zwit-EYYK bundle displays 16 solvent-exposed tyrosine side chains on the outside surface of the bundle superstructure. Close examination of the structure suggested that each phenolic hydroxyl group could be replaced by a boronic acid substituent without affecting bundle stability (Figure 1A).

To test this hypothesis and evaluate the polyol recognition potential of functionalized  $\beta$ -peptide bundles, we synthesized the monomeric sequences EBYK, EYBK, and EBBK, which each contain a boronic acid in place

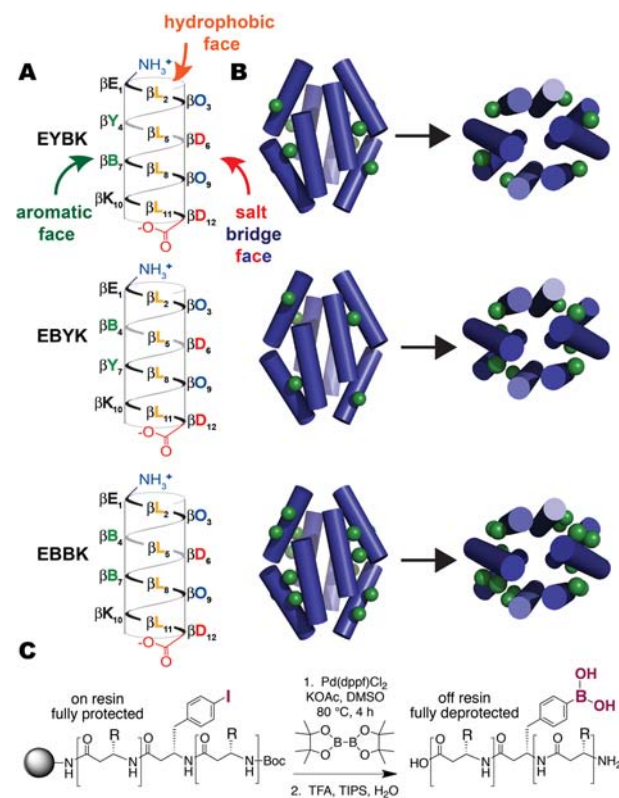


**Figure 1.** Structure and synthesis of  $\beta$ -borono-peptides EYBK, EBBK, and EBYK. (A) Sequences of  $\beta$ -borono-peptide monomers. B represents 4-borono- $\beta^3$ -homophenylalanine. (B) Cylinders show predicted location of phenylboronic acid (PBA) side chains (green) on the surface of an octameric bundle. (C) On-bead Miyaura reaction.

of one or both solvent-exposed tyrosine phenols (Figure 1). Once assembled into octameric bundles, these monomers would present either 8 (EYBK, EBYK) or 16 (EBBK) boronic acid functionalities capable of interacting with polyol ligands (Figure 1B).

The  $\beta$ -peptides EYBK, EBYK, and EBBK were prepared using solid phase methods, with the boronic acid functionality installed on-resin *via* a Miyaura reaction of the corresponding aryl iodide (Figure 1C).<sup>28</sup> The identities of  $\beta$ -peptide monomers EYBK, EBYK, and EBBK were verified by MALDI-TOF mass spectrometry using a dihydroxybenzoic acid matrix to minimize aggregation (Figure S1).<sup>29</sup>

Next we made use of circular dichroism (CD) spectroscopy to evaluate whether  $\beta$ -peptides EYBK, EBYK, and EBBK would assemble into oligomeric, 14-helical bundles of defined stoichiometry in solution. Despite the similarity at the level of the primary sequence, only the self-assembly of EYBK was well behaved (Figure S2). Like previously reported octameric bundles,<sup>24–27</sup> the CD spectrum of EYBK was characterized by minimal ellipticity between

(13) Musto, C. J.; Suslick, K. S. *Curr. Opin. Chem. Biol.* **2010**, *14*, 758.  
(14) James, T. D.; Samankumara Sandanayake, K. R. A.; Shinkai, S. *Nature* **1995**, *374*, 345.

(15) James, T. D.; Sandanayake, K. R. A. S.; Shinkai, S. *Angew. Chem., Int. Ed. Engl.* **1996**, *35*, 1910.

(16) Lorand, J. P.; Edwards, J. O. *J. Org. Chem.* **1959**, *24*, 769.

(17) Jin, S.; Cheng, Y.; Reid, S.; Li, M.; Wang, B. *Med. Res. Rev.* **2010**, *30*, 171.

(18) Pal, A.; Berube, M.; Hall, D. G. *Angew. Chem., Int. Ed.* **2010**, *49*, 1492.

(19) Ambrosi, M.; Cameron, N. R.; Davis, B. G. *Org. Biomol. Chem.* **2005**, *3*, 1593.

(20) Edwards, N. Y.; Sager, T. W.; McDevitt, J. T.; Anslyn, E. V. *J. Am. Chem. Soc.* **2007**, *129*, 13575.

(21) Badjic, J. D.; Nelson, A.; Cantrill, S. J.; Turnbull, W. B.; Stoddart, J. F. *Acc. Chem. Res.* **2005**, *38*, 723.

(22) Mammen, M.; Choi, S. K.; Whitesides, G. M. *Angew. Chem., Int. Ed.* **1998**, *37*, 2755.

(23) Knowles, R. R.; Jacobsen, E. N. *Proc. Natl. Acad. Sci. U.S.A.* **2010**, *107*, 20678.

(24) Daniels, D. S.; Petersson, E. J.; Qiu, J. X.; Schepartz, A. *J. Am. Chem. Soc.* **2007**, *129*, 1532.

(25) Petersson, E. J.; Craig, C. J.; Daniels, D. S.; Qiu, J. X.; Schepartz, A. *J. Am. Chem. Soc.* **2007**, *129*, 5344.

(26) Goodman, J. L.; Petersson, E. J.; Daniels, D. S.; Qiu, J. X.; Schepartz, A. *J. Am. Chem. Soc.* **2007**, *129*, 14746.

(27) Craig, C. J.; Goodman, J. L.; Schepartz, A. *ChemBioChem* **2011**, *12*, 1035.

(28) Afonso, A.; Rosés, C.; Planas, M.; Feliu, L. *Eur. J. Org. Chem.* **2010**, *2010*, 1461.

(29) Crumpton, J. B.; Zhang, W.; Santos, W. L. *Anal. Chem.* **2011**, *83*, 3548.

205 and 215 nm at concentrations as low as 5  $\mu\text{M}$  and a gradual increase in signal as the concentration was raised to 100  $\mu\text{M}$  (Figure S2A). By contrast, the CD spectra of EBYK showed lower levels of 14-helix structure, even at high concentration (Figure S2C), and that of EBBK was destabilized by  $\text{pH} \geq 5$  (Figure S3). The concentration dependent changes in the ellipticity of EBYK fit well to both a monomer–octamer equilibrium ( $\ln K_a = 85.1 \pm 0.4$ ;  $R^2 = 0.9648$ ) and a monomer–decamer equilibrium ( $\ln K_a = 109.9 \pm 0.6$ ;  $R^2 = 0.9489$ ) (Figure S2 and Table S2). Data from sedimentation equilibrium analytical ultracentrifugation (SE-AU) experiments were, however, uniquely consistent with an octameric assembly in solution ( $n = 7.98 \pm 0.26$ , RMSD = 0.00912) with an affinity constant ( $\ln K_a = 85.4 \pm 4.6$ , Figure S4) that matched the value estimated by CD. The fit of the SE-AU data to a monomer–decamer equilibrium was inferior (Table S2). The stability of the EBYK octamer is lower than that of the most stable bundle, EYYK ( $\ln K_a = 94.5$ ),<sup>27</sup> but higher than that of Zwit-1F ( $\ln K_a = 71.0$ ).<sup>24</sup>

Additional evidence for formation of a well folded EYBK bundle was provided by temperature-dependent CD studies, which revealed, as expected, that the thermal stability of the EYBK bundle depends on concentration (Figure S2B). These thermodynamic data indicate the extent to which phenylboronic acids are tolerated on the bundle surface. The sequence-dependent effects of the boronic acids on  $\beta$ -peptide bundle formation are likely due to their relative positions within the octameric structure (Figure 1A). The pH-dependent stability of EBBK may reflect a favorable interaction between adjacent phenylboronic acids within the  $\beta$ -bundle that counteracts the destabilizing effect of substitution at position 4.

We next solved the structure of the EYBK bundle using X-ray crystallography to unambiguously define both the oligomerization state and the molecular environment surrounding the phenylboronic acid side chains. The refined structure at 1.34 Å resolution ( $R/R_{\text{free}}$  14.6/18.6%) depicts an octameric bundle with the characteristic ‘palm-to-palm’ helical fold of all previously reported  $\beta$ -peptide bundles containing leucine-rich hydrophobic cores, including Zwit-EYYK.<sup>24–27</sup> The asymmetric unit comprises four 14-helices (RMSD < 0.4 Å) arranged in a parallel/anti-parallel/parallel array; this unit (one palm) assembles as a dimer with a leucine-rich hydrophobic core and with side chains comprising the EYBK motif exposed to the solvent (Figure 2A). The electron densities of all eight PBA side chains are well resolved (see Figure S5). The electron density of boron itself is weak, but the positions of the attendant hydroxyl oxygen atoms are clearly consistent with  $sp^2$  hybridization.

The eight phenylboronic acid (PBA) side chains on the EYBK bundle segregate into two environments that differ in both electrostatics and accessibility (Figure 2B). Type 1 PBAs, located on helices *b*, *c*, *f*, and *g*, lie at the interface of two parallel 14-helices. The pendant boronic acid points toward the salt bridge face of the adjacent helix. Type 2 PBAs, located on helices *a*, *d*, *e*, and *h*, lie near the C-terminus of a nearby helix (Figure 2C). To compare the two environments, we modeled the boronic acids as

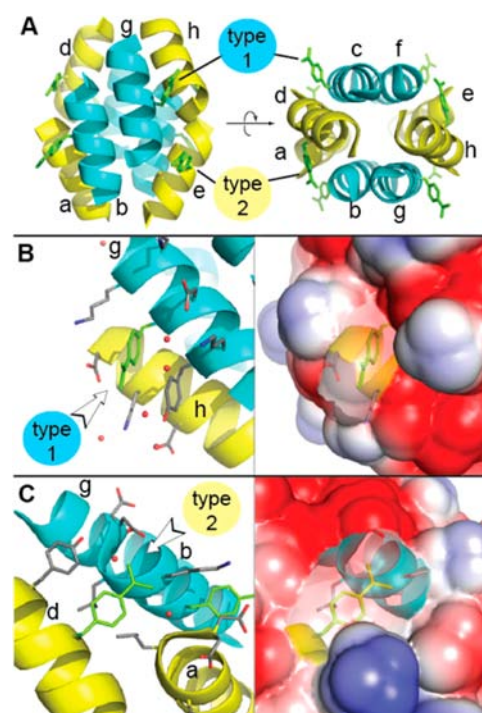


**Figure 2.** The EYBK  $\beta$ -peptide bundle structure as determined by X-ray crystallography. (A) Ribbon representation of the 14-helices the comprise each bundle with each of eight PBA side chains shown explicitly. Type 1 and 2 PBAs are appended to helices in blue and yellow, respectively. (B) Left: Type 1 PBA (green) on helix *g* faces solvent, in proximity to a salt bridge on adjacent helix *h*. An analogous environment exists on helices *b*, *c*, and *f*. Right: The electrostatic surface potential of a Type 1 site. (C) Left: Type 2 PBA (green) on helix *d* is located near the C-terminal carboxylic acid of adjacent helix *b*. An analogous environment exists on helices *a*, *e*, and *h*. Right: The electrostatic surface potential of a Type 2 site. Potentials shown assume a boronate ester. Potentials range from  $-50$  mV (red) to  $+50$  mV (blue).

boronate esters using charges and radii reported by Tafi *et al.*<sup>30</sup> At a Type 1 site, the overall negative potential is partially mitigated by two  $\beta$ -ornithine residues on the proximal salt bridge face. By contrast, at a Type 2 site, a cluster of nearby  $\beta$ -lysine residues provide intense regions of positive potential, offsetting the predominately negative potentials to a greater extent than found at the Type 1 sites. The two sites differ in accessibility as well: As calculated using the UCSF Chimera package,<sup>31</sup> Type 1 boronic acids are characterized by significantly higher solvent accessible surface areas than Type 2 boronic acids, 69.891 vs 49.224 Å<sup>2</sup>, respectively. The eight boronic acids on the bundle surface are organized into four pairs. Each pair consists of a Type 1 and a Type 2 PBA side chain spaced 12 Å apart (Figure S5C).

We next evaluated the capacity of the EYBK bundle to collect various polyols as part of their structure, using

(30) Tafi, A.; Agamennone, M.; Tortorella, P.; Alcaro, S.; Gallina, C.; Botta, M. *Eur. J. Med. Chem.* **2005**, *40*, 1134.

(31) Pettersen, E. F.; Goddard, T. D.; Huang, C. C.; Couch, G. S.; Greenblatt, D. M.; Meng, E. C.; Ferrin, T. E. *J. Comput. Chem.* **2004**, *25*, 1605.

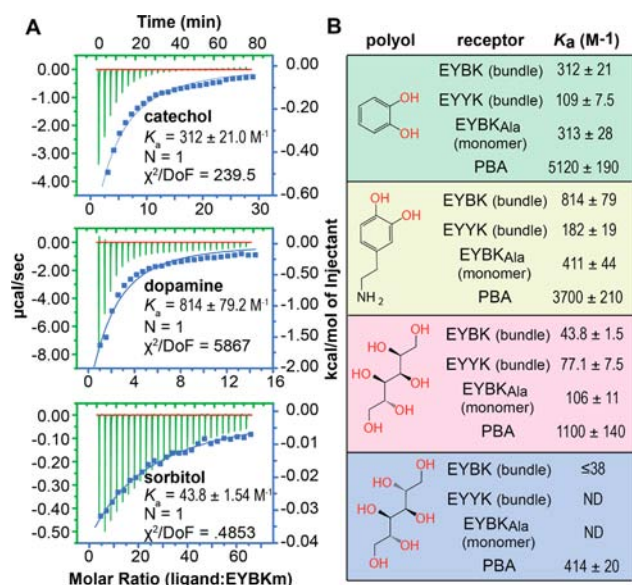


**Figure 3.** ITC data for selected EYBK-diol interactions at 25 °C in 30 mM phosphate buffer, pH 8. (A) ITC output shown in green. Integrated heat per injection shown in blue. Data was fit to a one-site model assuming  $n = 1$  and does not permit differentiation of Type 1 and Type 2 affinities. (B) Equilibrium association constants as determined by ITC.

isothermal titration calorimetry (ITC). While using ITC to determine thermodynamic parameters ( $\Delta H$ ,  $T\Delta S$ ) of weak interactions (where the Wiseman constant  $c < 1$ ) is uncommon, values of  $\Delta G$  (and thus  $K_a$ ) can be accurately determined.<sup>32</sup> Indeed, ITC analysis of the interactions between phenylboronic acid and various polyol and monosaccharides led to  $K_a$  values comparable to those measured by fluorescence (Table S4).<sup>33</sup> ITC was then used to examine the interactions between various monosaccharides and diols and the assembled EYBK bundle (Figure 3 and Table S5).

Several trends emerge from the data set. First, the monosaccharide/polyol affinities of the EYBK bundle are, with one exception, lower than values determined for PBA in a common aqueous buffer solution and corrected for stoichiometry on a “per-boron” basis. For the monosaccharide fructose, for example, no association with the EYBK bundle was detected using ITC (data not shown); the  $K_a$  values for the fructose·PBA complex is 97 M<sup>-1</sup>. The affinities of the polyols catechol and sorbitol for the EYBK bundle are 16- and 25-fold lower, respectively, than their affinities for PBA. As expected, the affinity of catechol and sorbitol for the EYBK bundle is comparable to the affinity

for an analog of EYBK (EYBK<sub>ala</sub>) that is constitutively monomeric and does not assemble into a supramolecular octameric complex.

We hypothesized that the lower polyol affinity of the EYBK bundle relative to PBA could be due to the negative electrostatics of both Type 1 and Type 2 sites or their limited solvent accessibility. To discriminate between these possibilities, we examined the affinity of PBA and the EYBK bundle for dopamine, a polyol distinguished by an amine that would be protonated at physiological pH ( $pK_a = 8.9$ ). The affinities of dopamine for EYBK and PBA differ by only a factor of 4, suggesting that the negative potential surrounding each boronic acid substituent in EYBK contributes to the lower affinity observed for catechol and sorbitol. It is interesting that the affinity of dopamine for the monomeric EYBK<sub>ala</sub>  $\beta$ -peptide is significantly lower than the affinity for EYBK bundle. This observation could suggest a unique interaction between dopamine and the array of functionality that defines the EYBK bundle in three dimensions.

A second emergent trend is that the bundle itself—not the boronic acids *per se*—contributes the majority of binding free energy to the polyol complexes evaluated. In the case of catechol and sorbitol, the affinity for the EYBK bundle exceeds that for the EYYK bundle, which lacks boronic acid, by only 3- and 1.7-fold, respectively, while in the case of dopamine the preference for the EYBK bundle is a factor of 4.5. The basis for these associations is not presently understood.

In summary our results demonstrate that the EYBK  $\beta$ -peptide can assemble into a folded quaternary structure and bind the polyol metabolites dopamine and sorbitol in neutral solution. The structure of this supramolecular complex identifies two distinct chemical environments that could be exploited in future designs for selective binding and/or catalysis. The Type 2 site is particularly promising, as it may provide the opportunity for carbohydrate–aromatic interactions.<sup>34</sup>

**Acknowledgment.** We thank Sunil Kumar for assistance with the ITC experiments. A.S. and S.J.M. are grateful to the W. M. Keck Foundation for support of this work. A.W. was supported in part by NSF DGE-1122492. J.C. was supported in part by the Camille and Henry Dreyfus Foundation.

**Supporting Information Available.** Experimental procedures and supplementary data. This information is available free of charge via the Internet at <http://pubs.acs.org>.

(34) Luis Asensio, J.; Arda, A.; Javier Canada, F.; Jimenez-Barbero, J. *Acc. Chem. Res.* **2013**, *46*, 946.

The authors declare no competing financial interest.

(32) Turnbull, W. B.; Daranas, A. H. *J. Am. Chem. Soc.* **2003**, *125*, 14859.

(33) Springsteen, G.; Wang, B. *Tetrahedron* **2002**, *58*, 5291.